

# Hybrid Optimization Algorithm Based on Whale Optimization and Fuzzy Logic for Magnetorheological Dampers

## Algoritmo híbrido de optimización de la ballena y la lógica difusa para amortiguadores magnetoreológicos

Verónica Valencia-Valencia<sup>1</sup>  Luis A. Lara-Valencia<sup>1</sup>  

<sup>1</sup>Universidad Nacional de Colombia. Núcleo Robledo. Medellín Colombia.

### Abstract

**Introduction:** to mitigate vibrations in structures subjected to dynamic loads, magnetorheological (MR) dampers have been studied as an effective solution to reduce the forces and deformations caused by these loads. Due to their highly nonlinear behavior, it is necessary to implement nonlinear control algorithms to achieve optimal control forces that minimize the response of the structures.

**Objective:** this study aims to reduce the response of a real building located in Medellín, Colombia, equipped with MR dampers. The goal is to optimize a fuzzy logic controller, using Gaussian membership functions that will be enhanced through the whale optimization algorithm, to find the appropriate voltage to be applied to the damper and generate optimal damping forces.

**Results:** the results show that the implementation of a set of MR dampers, controlled by fuzzy logic and optimized with the whale algorithm, significantly reduces the structural response to seismic loads. Reductions of 68% in displacement, 42% in velocity, 12% in acceleration, 42% in interstory drift, and 75% in the RMS value of displacement were observed compared to a system without control.

**Conclusions:** the application of the proposed controller proves to be effective in enhancing the performance of magnetorheological dampers in reducing the structural response to dynamic loads, highlighting its potential in the design of control systems for vibration mitigation in buildings.

**Keywords:** control of structures, Dynamic of structures, Fuzzy logic, Magnetorheological damper, Whale optimization algorithm

### How to cite?

Valencia-Valencia, V., Lara-Valencia, L.A., Hybrid Optimization Algorithm Based on Whale Optimization and Fuzzy Logic for Magnetorheological Dampers. Ingeniería y Competitividad, 2024, 26(3) e-20614128

<https://doi.org/10.25100/iyc.v26i3.14128>

Recibido: 21-05-24

Evaluado: 04-07-24

Aceptado: 29-08-24

Online: 23-09-24

### Correspondence

vvalenciav@unal.edu.co  
Carrera 80 N.º65-223. Medellín  
Colombia.



## Resumen

**Introducción:** para mitigar las vibraciones en estructuras sometidas a cargas dinámicas, se han estudiado los amortiguadores magnetoreológicos (MR) como una solución eficaz para reducir las fuerzas y deformaciones causadas por estas cargas. Debido a su comportamiento altamente no lineal, es necesario implementar algoritmos de control no lineales para lograr fuerzas de control óptimas que minimicen la respuesta de las estructuras.

**Objetivo:** este estudio tiene como objetivo reducir la respuesta de un edificio real ubicado en Medellín, Colombia, equipado con amortiguadores MR. Se busca optimizar un controlador de lógica difusa, utilizando funciones de membresía Gaussianas que serán mejoradas mediante el algoritmo de optimización de la ballena, para encontrar el voltaje adecuado que debe aplicarse al amortiguador y generar fuerzas de amortiguación óptimas.

**Resultados:** los resultados muestran que la implementación de un conjunto de amortiguadores MR, controlados por lógica difusa y optimizados con el algoritmo de la ballena, reduce significativamente la respuesta estructural ante cargas sísmicas. Se observaron reducciones del 68% en desplazamiento, 42% en velocidad, 12% en aceleración, 42% en la deriva entre pisos y 75% en el valor RMS de desplazamiento en comparación con un sistema sin control.

**Conclusiones:** la aplicación del controlador propuesto demuestra ser efectiva para mejorar el rendimiento de los amortiguadores magnetoreológicos en la reducción de la respuesta estructural ante cargas dinámicas, lo que resalta su potencial en el diseño de sistemas de control para la mitigación de vibraciones en edificaciones.

**Palabras clave:** control de estructuras, Dinámica de estructuras, Lógica difusa, Amortiguador magnetoreológico, Algoritmo de optimización de la ballena

### Why was it conducted?:

This study was conducted to improve the performance of magnetorheological (MR) dampers in structures under different seismic conditions. The main objective was to optimize the voltage input to the dampers to achieve optimal damping forces and reduce the structural response during seismic events. To achieve this, the Whale Optimization Algorithm (WOA) was used to optimize the parameters of Gaussian membership functions in a Fuzzy Logic Control (FLC) system. The integration of these methods aimed to enhance the nonlinear control of the MR dampers.

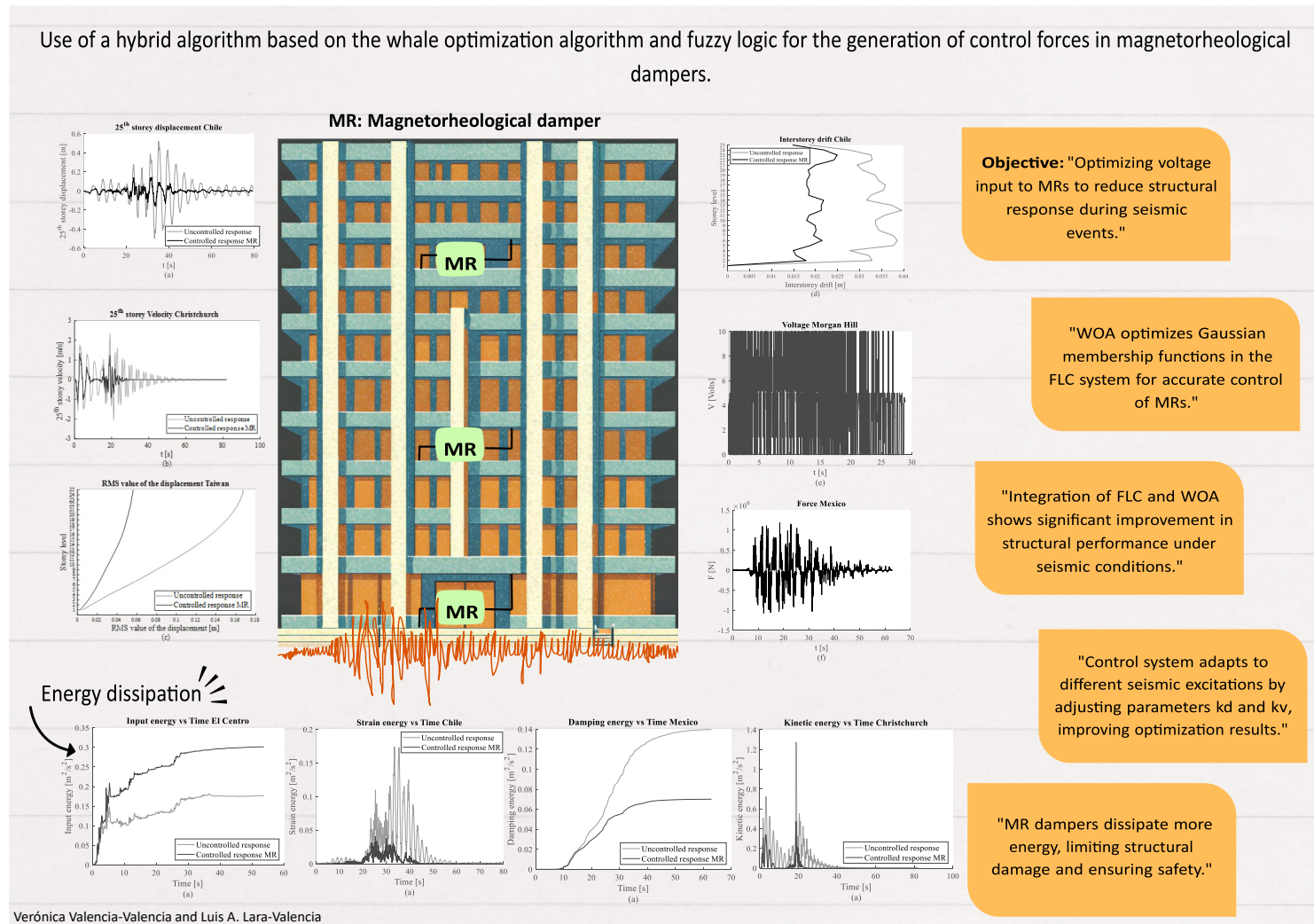
### What were the most relevant results?

The most relevant results include significant reductions in various structural response parameters when compared to uncontrolled structures, such as: displacement reduction of up to 68%, velocity reduction of up to 42%, acceleration reduction of up to 12%, interstory drift reduction of up to 42%, RMS value of displacement reduced by up to 75%. Additionally, the control system demonstrated adaptability to different seismic excitations by adjusting key scaling factors  $k_d$  and  $k_v$ . The study also showed that MR dampers dissipate more energy than uncontrolled cases, improving overall safety and limiting structural damage.

### What do these results contribute?

These results contribute significantly to improving the control of structural responses in buildings under seismic loads, demonstrating that the integration of MR dampers with an optimized FLC system using WOA is effective in reducing displacements, velocities, accelerations, and interstory drifts. The flexibility of the system to adapt to different seismic excitations and its high efficiency in dissipating energy enhance its ability to mitigate structural damage and improve the overall safety of structures during seismic events.

## Graphical Abstract



## Introduction

The vibrations in structures produced by dynamic loads can be controlled using structural control systems that are used to decrease and dissipate the energy of structures produced by these loads like seismic excitations (1,2). Semi-active control systems are control devices that can regulate a structure when it is subjected to a seismic load, using less energy than an active control system and using the inherent reliability of a passive control system (3–6). These controllers use the response of the structure to calculate control forces aimed at reducing the response during seismic events (7,8). Among the semi-active control systems is the magnetorheological (MR) damper. The MR damper is a semi-active controller that employs a controllable MR fluid that can manage vibrations in real-time (9). The fluid contains magnetized polarizable particles in an oily medium and it is controlled by a magnetic field; when it appears, the fluid works like a semisolid liquid because the field increases the resistance, and without it, the fluid flows like a liquid (10–12). In 1996, Dyke et al. (13) presented an optimal control strategy to reduce structural responses during seismic loads using MR controllers. In 1997, Spencer et al. (14) introduced the non-linear phenomenological model of MR damper. This model is based on a modified Bouc-Wen hysteresis model intended to be computationally tractable

while still displaying hysteretic tendencies (15). MR dampers take advantage of the properties of MR fluids, which can change rapidly when exposed to a magnetic field. As a result, these dampers can modify damping forces efficiently and safely, demonstrating their remarkable hysteresis capabilities (16–18). However, the strong nonlinear behavior of MR dampers is one of the significant issues they provide. As a result, it is critical to design a suitable controller that tries to maximize force output while minimizing power consumption (19). Therefore, it is necessary to work on non-linear control algorithms derived from mathematical formulations or intelligent methods based on neural networks (20–22), fuzzy logic (23–25), and multiple regression models (26).

Researchers also studied how to design and optimize MR dampers. Ding et al. (27) presented an innovative design featuring bidirectional adjusting damping forces to enhance the fail-safe property of the MR damper. Additionally, they proposed a Gompertz model to describe the nonlinear hysteretic behavior of the device. In 2021, Wani et al. (28) proposed an experimental and numerical study that figured out the efficiency of multiple response optimization control using an MR damper for mitigating the structural response. Diptesh et al. (29) formulated a fuzzy logic control (FLC) algorithm that uses MR damper characteristics without needing a Bouc-Wen Model approach that involves the fuzzification of the MR damper properties.

On the other hand, metaheuristic algorithms are applied to some hard optimization problems and imitate features in nature to overcome the limitations of some classical methods (30). These methods try to make a robust algorithm for the fast solving of significant problems and are quite easy to use and implement in any work, also they are sectioned into single-solution-based and population-based metaheuristic algorithms (31). The Bat algorithm (BA) is based on Bat's echolocation to avoid obstacles, detect their nests in the dark, and locate food and prey, they fly randomly with velocity, direction, and frequency, changing their wavelength and loudness to search for food and preys (32–34). Bekdas et al. (35) presented a novel optimization using the BA for improving the response of structures using tuned mass dampers. The Grey wolf algorithm (GWO) uses the wolf hierarchy, where the alpha leads the hunt followed by the beta and delta, and the omegas search for the prey. The idea is to find the best solutions by updating the position of the other members (36–38). In 2021, Takin et al. (39) applied MR dampers to a building using a fuzzy algorithm and selected the location of the dampers using a GWO. The Whale optimization algorithm (WOA) is developed based on the social behaviors of humpback whales that use a bubble net strategy when hunting fish, when they decide which whale has the best solution, the other whales update their positions (40–42). Lin et al. (42) proposed a control strategy for adjacent structures using MR dampers using an FLC for the allocation and the dampers were designed using WOA. The Cuckoo search algorithm (CS) is inspired by the reproduction of cuckoo birds and their aggressive breeding strategy, the algorithm tries to find the best solution when each bird finds a nest to lay its egg with a higher chance to hatch (43–45). Rosli et al. (46) proposed a Bouc-Wen hysteresis parameter optimization for MR dampers using the CS algorithm for optimization.

This study focuses on improving the performance of a set of MR dampers in a mid-rise building under different seismic conditions. The main objective is to optimize the voltage input to the dampers to achieve the optimal damping forces to reduce the structural response during seismic events. To accomplish this, the study employs the WOA to optimize the parameters of the Gaussian membership functions used in the FLC system. This integration between FLC and WOA enables the identification of accurate parameters in this non-linear control system, leading to improved control strategies for the MR dampers. Additionally, the study evaluates the dissipated energy to provide a comprehensive assessment of system performance.

## Methodology

### The dynamic problem in terms of the space-state equation

Eq (1) states the dynamic equilibrium of a  $n$  degrees of freedom system. In this equation,  $M$ ,  $C$ , and  $K$  represent mass, damping, and stiffness, respectively. The vectors  $\mathbf{x}$ ,  $\dot{\mathbf{x}}$ , and  $\ddot{\mathbf{x}}$  indicate the relative

displacement, velocity, and acceleration of the structure, respectively. The vector  $f$  represents the imposed loads, while  $w$  represents control forces acting on the structure.  $E$  and  $D$  are the matrices where the external forces and the control forces are located (47).

$$M\dot{x}(t) + Cx(t) + Kx(t) = Dw(t) + Ef(t) \quad (1)$$

The dynamic system will be given as a collection of first-order differential equations called the state-space representation. This simplifies the manipulation of some mathematical expressions. Eqs (2) and (3) illustrate this transformation into a state-space equation for convenience, where matrices  $A$ ,  $B$ , and  $H$  are presented in Eqs (4), (5), and (6) respectively. Where  $\mathbf{0}$  is a zero matrix ( $n \times n$ ) and  $\mathbf{I}$  is the identity matrix ( $n \times n$ ).

$$z(t) = \begin{bmatrix} x(t) \\ \dot{x}(t) \end{bmatrix} \quad (2)$$

$$\dot{z}(t) = Az(t) + Bw(t) + Hf(t) \quad (3)$$

$$A = \begin{bmatrix} \mathbf{0} & \mathbf{I} \\ -M^{-1}K & -M^{-1}C \end{bmatrix} \quad (4)$$

$$B = \begin{bmatrix} \mathbf{0} \\ M^{-1}D \end{bmatrix} \quad (5)$$

$$H = \begin{bmatrix} \mathbf{0} \\ M^{-1}E \end{bmatrix} \quad (6)$$

#### Phenomenological model of magnetorheological dampers

Spencer et al. (14) suggested a parametric phenomenological model to enhance the replication of the force-velocity behavior of MR dampers. Figure (1) represents the modified Bouc-Wen model, which incorporates the original Bouc-Wen model and introduces a spring connected in parallel to the entire system, increasing its stiffness. Additionally, an extra damper is integrated in series. This modification enhances the overall performance of the Bouc-Wen model, making it a more versatile and accurate representation of the system.

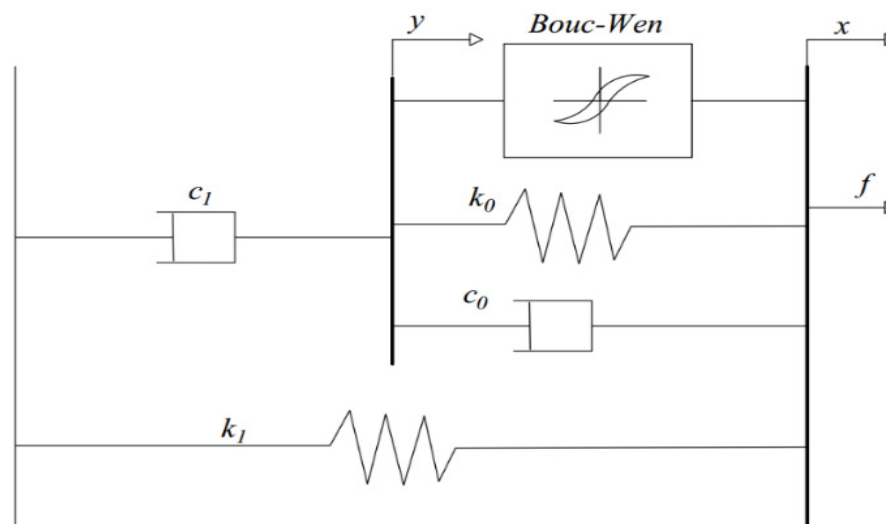


Figure 1: Phenomenological model



The force produced by the controller in this model is governed by Eq (7). The parameter  $x_0$  represents the initial displacement of the spring;  $x$ , denotes the relative displacement at one end of the damper;  $\dot{x}$ , the damper speed;  $z$ , the evolutionary variable presented in Eq (8);  $c_0$  and  $c_1$  denote the viscous damping at high and low speeds respectively;  $k_0$ , is the stiffness of the damper at high speeds, and  $k_1$ , represents the stiffness of the damper. Additionally, parameters  $\gamma$ ,  $\beta$ , and  $A$  determine the shape of the hysteresis cycle and are constant values, while  $\alpha$  and  $n$  regulate the internal state  $z$  and its evolution in relation to the force  $f$  (47). The parameter  $y$  is the internal displacement of the damper. However, is important to note that this parameter is theoretical and does not correspond to any actual physical displacement within the MR damper (48).

$$f = \alpha z + c_0 (\dot{x} - \dot{y}) + k_0 (x - y) + k_1 (x - x_0) \quad (7)$$

$$z = -\gamma |\dot{x} - \dot{y}| |z| |z|^{n-1} - \beta (\dot{x} - \dot{y}) |z|^n + A (\dot{x} - \dot{y}) \quad (8)$$

Eq (9) defines  $\dot{y}$ .

$$\dot{y} = \frac{1}{(c_0 + c_1)} [\alpha z + c_0 \dot{x} + k_0 (x - y)] \quad (9)$$

Additionally, values  $\alpha$ ,  $c_0$ , and  $c_1$  are voltage-dependent (49) and their formulations are shown in Eqs (10), (11), and (12).

$$\alpha = \alpha_a + \alpha_b u \quad (10)$$

$$c_0 = c_{0a} + c_{0b} u \quad (11)$$

$$c_1 = c_{1a} + c_{1b} u \quad (12)$$

Where  $\alpha_a$ ,  $\alpha_b$ ,  $c_{0a}$ ,  $c_{0b}$ ,  $c_{1a}$ , and  $c_{1b}$  are fixed parameters that are connected between the force of the damper and the voltage determined through experimental results. Furthermore, the dynamics implicated in the MR fluid achieving rheological equilibrium are modeled by the first-order filter shown in Eq (13):

$$\dot{u} = -\eta(u - v) u \quad (13)$$

Where  $u$ ,  $v$ , and  $\eta$  are the input voltage, output voltage, and the time constant for the first-order filter, respectively.

### Whale optimization algorithm (WOA)

In 2016, Mirjalili and Lewis (40) introduced the WOA, a meta-heuristic optimization method inspired by the social behavior of humpback whales and their distinctive bubble-net feeding technique. The main strategy of this algorithm involves creating a population of whales, which is equivalent to a set of random solutions. Each solution is linked to a whale that tries to find a new location in the searching space, with the best-performing whale in the group serving as a reference point for the others (50).

The initial strategy used by the algorithm mimics the bubble-net attacking method, also known as the exploitation phase. This behavior involves the whales creating a spiral of bubbles around their prey before swimming up to the surface (51). At this moment, the mathematical model uses two methods: encircling and the formation of bubble nets by spiral updating, therefore the probability that they will employ either of the two listed techniques is equal.

In the encircling method, the whales find the positions of both the target and the prey and proceed to encircle them. At first, not all the whales have the optimal strategy for identifying the prey within

the search area. Instead, the whale closest to the optimal response is expected to reveal it from the top candidate. By profiling this top-performing search agent, the remaining search agents adjust their approaches to coordinate with the best agent's direction (52). This strategy can be represented by Eqs (14) and (15):

$$\Delta = |C' \cdot X_i^* - X_i| \quad (14)$$

$$X_{i+1} = X_i - A' \cdot \Delta \quad (15)$$

Where  $X_i^*$  is the optimal solution provided within the vector of position denoted as  $X$ ,  $\Delta$  is the distance between the whale and the prey,  $i$  is the current iteration, and  $A'$  and  $C'$  are coefficient vectors calculated as presented in Eqs (16) and (17), respectively.

$$A' = 2a \cdot r - a \quad (16)$$

$$C' = 2 \cdot r \quad (17)$$

In this context, the vector  $r$  is arbitrarily selected between [0, 1], while the value of  $a$  is systematically decreased from 2 to 0 during the exploitation and exploration phases.

When forming bubble nets through spiral updating, the method presents two choices: selecting a random search agent when  $A' \geq 1$  or opting for the best solution to update the positions of the agents when  $A' < 1$ . The selection between an encircling mechanism or a spiral model is assumed to be equally probable, aiming to enhance the positions of the search agents and bring them closer to the optimal solution during the optimization process (53). This process is mathematically formulated as shown in Eq (18) and (19):

$$X_{i+1} = \begin{cases} X_i^* - A' \cdot \Delta & \text{if } p < 0.5 \\ \Delta' \cdot e^{bl} \cdot \cos(2\pi l) + X_i^* & \text{if } p \geq 0.5 \end{cases} \quad (18)$$

$$\Delta' = |X_i^* - X_{i|l}| \quad (19)$$

Where  $\Delta'$  defines the distance between the whale and the prey,  $p$  is an arbitrary number between [0, 1],  $b$  characterizes the spiral shape, and  $l$  is a random number between [0, 1].

Another strategy the algorithm uses is the search of the prey or exploration phase. To hunt, whales encircle their prey and adjust their position to achieve the best outcome. The target prey is considered the current best candidate solution, with the whale position updated according to a randomly chosen search agent rather than the best solution available at that moment. To make this phase possible, the current whale can search far from the best solution, and the WOA can do a global search while avoiding local minima (54). This formulation uses the same Eqs (14) and (15) but  $X_i^*$  changes for a random value  $X_{rand}$ .

### Fuzzy logic control (FLC)

Zadeh (55) first proposed fuzzy logic, linking fuzzy implication and compositional inference rules with linguistic control rules via a fuzzy logic controller. FLC is a rule-based system, ideal for complex and dynamic systems due to its ambiguity and uncertainty. It relies on a well-structured database that has linguistic control rules that specify the relationships between input and output variables. FLC requires a fuzzification interface to transform real-world data into fuzzy data for system management. Its decision-making inference system uses the knowledge base to form logical inferences based on fuzzy input data and established criteria. In the inference process, ambiguous inputs are effectively translated into proper control actions. Finally, a defuzzification interface converts the fuzzy control action output into a concrete, actionable control action (51). Fuzzy systems operate based on membership functions and fuzzy control rules, with membership functions indicating how well an element fits into a specific set.

The purpose of the controller based on the concepts described by Liu et al. (56), is to maintain the structure at an equilibrium position. If the structure deviates, the controller increases the voltage to enhance damping and stabilize the structure. Conversely, when the structure approaches the equilibrium point, the controller decreases or ceases voltage delivery, as it is no longer necessary. Liu et al. (56) proposed seven Gaussian membership functions for the fuzzification interface to define displacement and velocity inside the range  $[-1, 1]$ . These functions assign a degree of membership to each displacement and velocity value based on their proximity to the linguistic variables. Scale factors,  $n_d$  and  $n_v$  for displacement and velocity respectively, are also required. The formulas for calculating these parameters are provided in Eqs (20) and (21):

$$n_d = k_d x \quad (20)$$

$$n_v = k_v \dot{x} \quad (21)$$

These equations utilize the input variables  $x$  and  $\dot{x}$  for displacement and velocity on the first floor of the building, incorporating scaling coefficients  $k_d$  and  $k_v$  for displacement and velocity, respectively. As outlined in Table (1), the inference system of the controller consists of seven fuzzy rules that utilize linguistic terms negative large (NL), negative medium (NM), negative small (NS), zero (ZO), positive small (PS), positive medium (PM), and positive large (PL) (56).

Table 1. FLC inference system

	NL	NM	NS	ZO	PS	PM	PL
NL	PL	PL	PL	PM	ZO	ZO	ZO
NM	PL	PL	PL	PS	ZO	ZO	PS
NS	PL	PL	PL	ZO	ZO	PS	PM
ZO	PL	PM	PS	ZO	PS	PM	PL
PS	PM	PS	ZO	ZO	PL	PL	PL
PM	PS	ZO	ZO	PS	PL	PL	PL
PL	ZO	ZO	ZO	PM	PL	PL	PL

The output voltage is calculated using four Gaussian membership functions, (ZO, PS, PM, and PL) with values between  $[0, 1]$ . These functions use the centroid method to figure out voltage values. Eq (22) is used to change the output voltage from a fuzzy control action to a real control action between 0 and 10 V (57), and  $V$  is the damper voltage to be applied and  $s$  is the FLC output value.

$$V = 10 \cdot \left( \frac{5}{3} s - \frac{1}{3} \right) \quad (22)$$

### Hybrid WOA-FLC algorithm

The WOA has shown to be an impressive tool for solving a variety of optimization issues. However, one of its problems is the long time it takes to reach the global optimum (58). To address this limitation FLC is used to enhance the obtained results. The mean value and the standard deviation to be used in the Gaussian membership functions, as shown in Eq (23), are specified by the WOA which gives random values for  $\mu$  and  $\sigma$ , then, these enhanced functions are used to improve the aspects of displacement, velocity, and voltage. Armed with these tailored settings, the FLC then calculates the necessary voltage and forces to be applied and sends the new results to the WOA's objective function.



$$f(x, \sigma, \mu) = e^{-\frac{|x - \mu|}{\sigma}} \quad (23)$$

The fundamental purpose of the algorithm is to have an objective function that tries to minimize the dynamic response of the structure under seismic excitations and optimize the structural performance. The study focuses on determining the lowest values of the RMS response for maximum displacements, aiming to enhance the overall stability of the structure against seismic events. The proposed objective function is critical in guiding the optimization process, ultimately leading to improved structural designs with lower dynamic reactions and increased seismic resistance. Finally, if the best value is generated, the algorithm adjusts the current best value and repeats the process until the given number of whales and generations are completed. The optimization process increases efficiency and accuracy because of this combined WOA-FLC strategy, fostering the pursuit of improved solutions in complex optimization scenarios. Figure (2) shows a diagram that represents how the hybrid WOA-FLC algorithm works in the control project proposed.

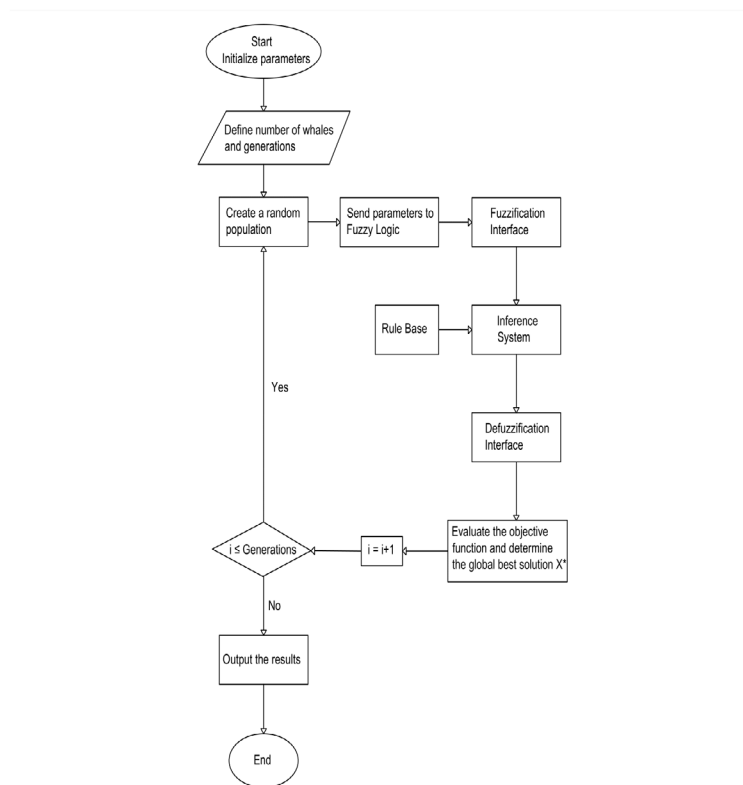


Figure 2. Hybrid WOA-FLC algorithm flowchart

### Case of study

Validating a case study is essential to prove the effectiveness of the control project proposed. For this purpose, a 25-floor building located in Medellin, Colombia was used as a case of study. The structure has the features of a medium-rise building and is 73 meters tall overall. Its lateral force-resisting system is made up of resistant moment frames. Following a trial-and-error analysis, it was considered that deploying three controllers on the 1st, 10th, and 20th floors stands out as one of the most effective methods for enhancing the overall performance of the entire system. [The case study is a plane frame presented along axis C](#) and the configuration of the structure is shown in Figure (3).

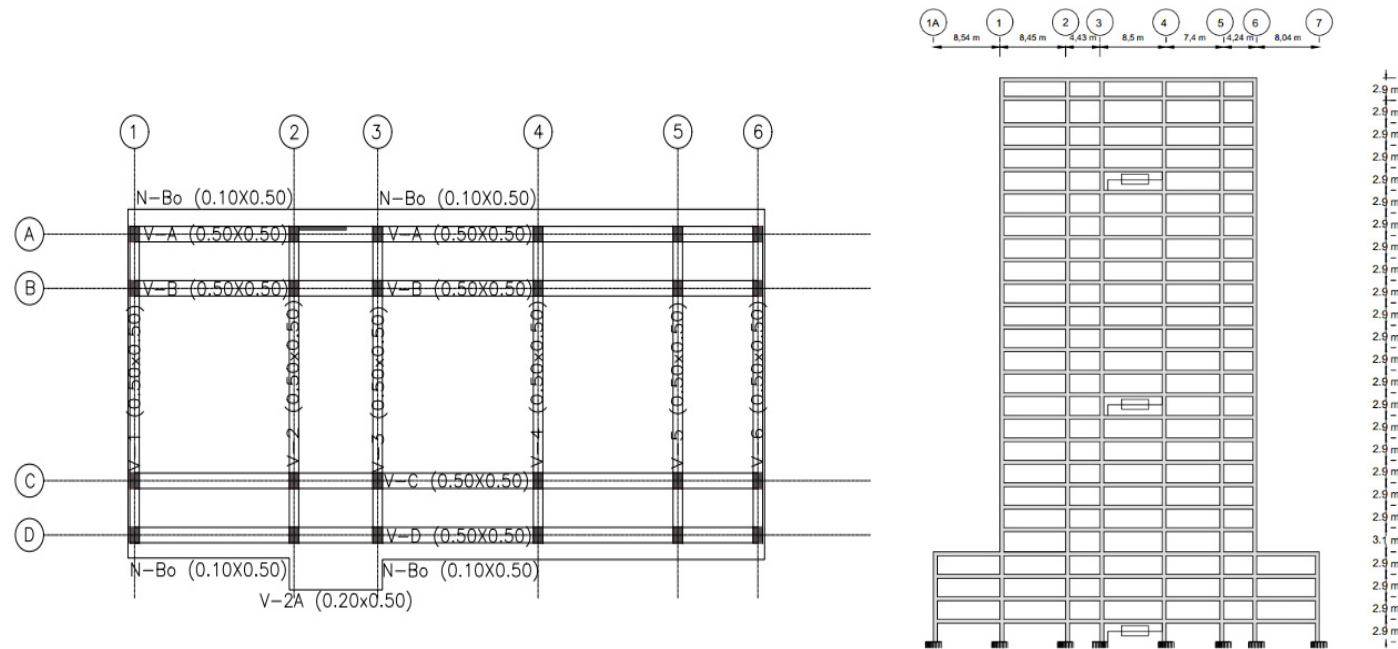


Figure 3. Configuration of the structure

By assuming that the floor diaphragms are infinitely rigid and using static condensation to reduce the rotational degrees of freedom, the stiffness matrix was simplified to a single degree of freedom per floor. Alongside the stiffness matrix, the mass matrix is utilized to calculate the structure's dynamic response. The mass matrix diagonal entries indicate the mass of each floor. Rayleigh damping was employed to determine the damping matrix, with 5.0% of critical damping ( $\xi$ ) applied to the structure's initial and final dynamic modes. Table (2) presents the parameters used for the phenomenological of the MR damper.

Table 2. Parameters of the MR device used. Modified from (59)

Parameters used in the phenomenological model			
$c_{0a}$	110 kN·s/m	$\alpha_a$	46.2 kN/m
$c_{0b}$	114.3 kN·s/m/V	$\alpha_b$	41.2 kN/m/V
$c_{1a}$	8359 kN·s/m	$\gamma$	164 1/m <sup>2</sup>
$c_{1b}$	7482.9 kN·s/m	$\beta$	164 1/m <sup>2</sup>
$k_0$	0.01 kN/m	$A$	1107.2
$k_1$	0.485 kN/m	$n$	2
$x_0$	0	$\eta$	100 1/s

The ability of the damper to decrease vibrations and enhance the overall stability of the structure

will be determined by analyzing and comparing the results obtained from eight different seismic excitations that were selected based on their magnitudes, durations, and locations to validate the effectiveness of the damper. This approach allows a comprehensive analysis of the response of the structure under different seismic scenarios. By using a diverse set of excitations, it is possible to study the behavior of the structure over a range of conditions, providing valuable insight into its dynamic performance and response characteristics. The excitations used in this work are listed in Table (3) and were acquired from the Center for Engineering Strong Motion Data (60). The table has details of each excitation, such as direction, peak ground acceleration (PGA), and duration of each excitation, as well as the place, year, and magnitude of the seismic event.

Table 3. Seismic excitations.

Event	Year	Station	Component	Magnitude	PGA [g]	Duration [s]
El Centro	1940	El Centro (117)	S90W	6.9	0.348	53.73
Central Chile	1985	Melipilla	0	7.8	0.686	79.36
Christchurch	2011	Christchurch Resthaven	S88E	6.3	1.039	81.90
Kobe	1995	CUE: Nishi-Akashi	90	6.9	0.503	41.00
Mexico	1985	La Union	S00E	8.1	0.169	62.93
Morgan Hill	1984	USGS	250	6.1	0.640	28.91
Petrolia	1992	Cape Mendocino, CA	90	7.0	0.710	59.98
Taiwan	1999	Taichung	90	7.6	1.010	159.99

## Results and discussion

The WOA was used to obtain the configurations for the FLC. This involved iteratively adjusting the membership functions for inputs and outputs to identify the optimal configuration that minimizes the fitness function. The FLC was then used to assess the dynamic reactions of the structure to eight different seismic excitations, armed with these adjusted parameters.

Different combinations of whales and generations were tested during the implementation of the WOA. The results demonstrated that using a larger number of whales resulted in more precise parameter optimization. This was linked to a larger population capacity of whales to explore a search space and avoid becoming locked in local optima. Notably, the study found that using 80 whales and 30 generations greatly decreased the controlled reaction throughout the optimization phase. However, it was discovered that different scaling coefficients,  $k_d$ , and  $k_v$ , were required for different seismic excitations to approach better results, as shown in Table (4). The WOA adapted to the individual characteristics of the seismic excitations, resulting in superior optimization results in each scenario.

Table 4. Scaling coefficients  $k_d$  and  $k_v$ .

Event	$k_d$	$k_v$
El Centro	500	70
Central Chile	400	70
Christchurch	500	70
Kobe	400	70
Mexico	400	70
Morgan Hill	500	70
Petrolia	400	70
Taiwan	700	75

In most seismic excitations, the values typically stay consistent; however, for Taiwan, there is an increase in the values for  $k_d$  and  $k_v$ . This phenomenon may be attributed to the higher PGA experienced in Taiwan, which persists over time, resulting in the need for elevated values of  $k_d$  and  $k_v$  to effectively respond to and mitigate the seismic forces exerted on the structures.

### Gaussians Membership Functions

The graphical representations of the Gaussian membership functions defined by FLC with WOA were created for the displacement, velocity, and voltage variables. They specifically exhibit seven fuzzy rules defined for displacement and velocity, as well as the four established voltage fuzzy rules. These graphics visually depict the relationship between the linguistic variables and their corresponding degrees of membership, highlighting the fuzzy logic control approach employed by the WOA. Figure (4) presents the Gaussian membership functions for Christchurch seismic excitation optimized using the metaheuristic methodology.

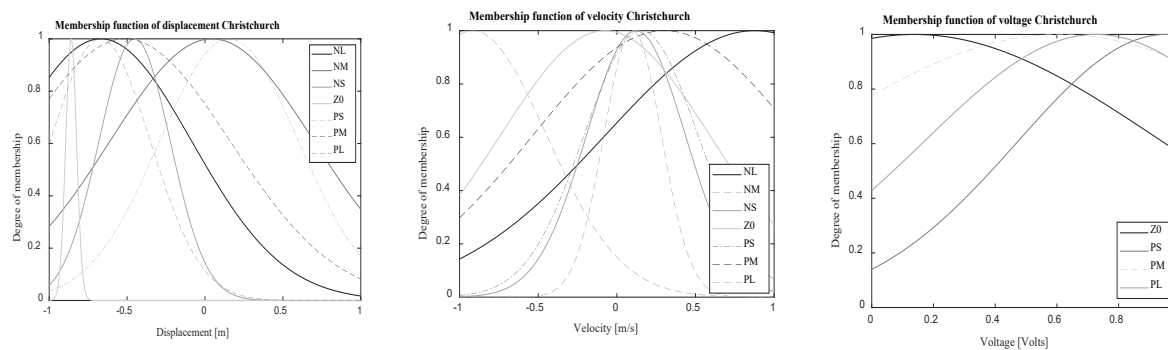


Figure 4. Membership functions in Christchurch.

### Uncontrolled and Controlled response

Results obtained for the response of the structure are in Table (5), showing the reductions for displacement, velocity, RMS value of displacement, and maximum interstory drift during different seismic excitations.

Table 5. Reductions of displacement, velocity, RMS value of displacement, and maximum drift.

Event	Displacement reduction [%]	Velocity reduction [%]	Acceleration reduction [%]	RMS value of displacement reduction	Maximum Drift reduction [%]
El Centro	31.15	15.70	6.19	39.06	17.89
Central Chile	68.74	42.11	11.96	75.58	42.20
Christchurch	29.82	42.23	27.43	54.57	27.29
Kobe	28.36	10.00	12.01	47.82	16.24
Mexico	39.36	19.66	2.02	56.37	24.86
Morgan Hill	50.70	24.79	19.20	56.10	22.56
Petrolia	11.33	25.48	7.66	40.66	17.42
Taiwan	41.24	34.76	6.10	66.27	28.29

MR dampers exhibit significant effectiveness in reducing displacement across different seismic events. Reductions range from 11.33% in Petrolia to 68.74% in Central Chile. Moreover, they demonstrate a notable reduction in velocity, ranging from 10.00% in Kobe to 42.23% in Christchurch. The RMS value of displacement provides an overall measure of effectiveness over the entire seismic event, with reductions ranging from 40.66% in Petrolia to 75.58% in Central Chile, indicating substantial effectiveness. The maximum interstory drift reduction is crucial for limiting structural

damage and ensuring occupant safety, ranging from 16.24% in Kobe to 42.20% in Central Chile, showing that the dampers effectively reduce the maximum drift experienced by the structure. This indicates that the dampers are effective in limiting the overall displacement and velocity of the structure under seismic loads.

The analysis of the different seismic excitations highlights the exceptional performance of the controller in the central Chile event. In this scenario, the structural response has the greatest reduction compared to other seismic events, particularly in terms of velocity and RMS value of displacement. This reduction indicates successful mitigation of the seismic excitation in the structure.

On the other hand, the case of the seismic excitation of Kobe exhibits the least reduction in velocity and interstory drift. In contrast, the performance of the controller for the Morgan Hill seismic excitation stands out for its remarkable reduction in displacement, RMS value of displacement, and interstory drift. However, the case where the seismic excitation of Mexico is noteworthy for requiring the least applied force, with the control system significantly reducing displacement, velocity, interstory drift, and RMS value of displacement. Finally, Petrolia and Taiwan, show significant reductions in all components. These findings underscore the effectiveness of various mitigation strategies in reducing the impact of seismic events on structures, with each seismic excitation presenting unique challenges and opportunities for improvement.

The maximum control forces developed by the MR dampers, as shown in Table (6), vary depending on the seismic event, ranging from 1181 kN in Mexico to 2277 kN in Taiwan, representing the maximum forces applied to the dampers to control the response of the structure during each event. The reason for Taiwan and Christchurch's high force requirements is probably that their PGA values are noticeably higher.

Figure (5) displays these results, highlighting some of the significant outcomes mentioned. It notably shows the reductions induced by the control device and illustrates the voltage ranging from 0 to 10 V during the excitation, along with the optimal force applied.

Table 6. Maximum Force developed by the MR dampers.

Event	Maximum control Force [kN]
El Centro	1585
Central Chile	1339
Christchurch	2130
Kobe	1473
Mexico	1181
Morgan Hill	1451
Petrolia	1783
Taiwan	2277



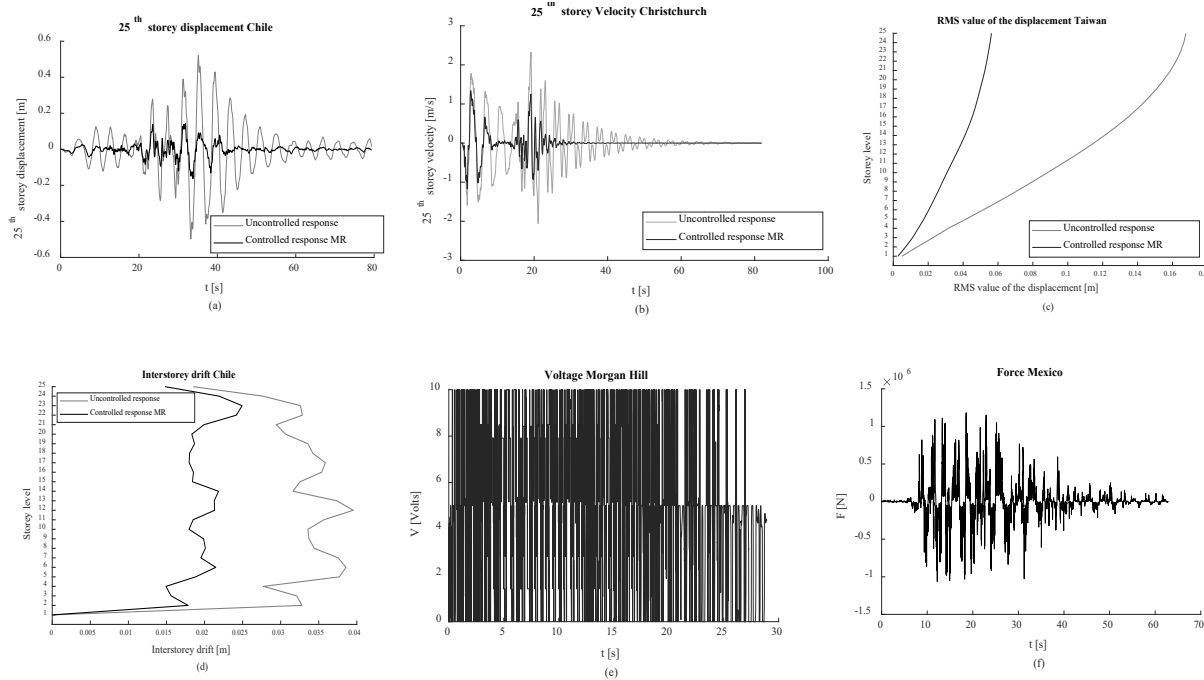


Figure 5: Response of the structure subjected to different seismic excitations. (a) 25th story maximum displacement in Chile. (b) 25th story maximum velocity in Christchurch. (c) RMS value of the displacement per story in Taiwan. (d) Maximum interstory drift in Chile. (e) Voltage in Morgan Hill. (f) Force in Mexico

### Energy curves

Analyzing the energy dissipation using dampers is one of the most efficient ways to confirm the effectiveness of a control system. In this case, were evaluated the input energy, strain energy, damping energy, and kinetic energy. The validation ensures the accuracy and dependability of control systems under assessment by examining and contrasting these elements. The performance and efficacy of control systems can be clearly and completely understood by conducting a thorough study of these energy-related factors.

Figure (6) shows the results obtained for the input energy. It is presented that the input energy is higher for the controlled response of the structure using the MR damper. This is possible because this semi-active controller injects energy, unlike passive controllers that don't require external energy.

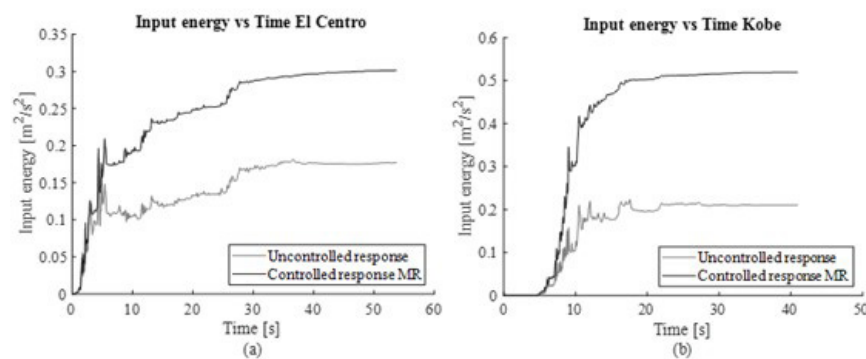


Figure 6. Input Energy. (a) Input Energy for El Centro. (b) Input Energy for Kobe.

The results show a significant reduction in the Strain Energy as shown in Figure (7). For the seismic excitation in Chile, the average reduction was 77%, one of the best reductions. In Taiwan, the reduction was around 50%, indicating that the dissipation of the strain energy was very effective.

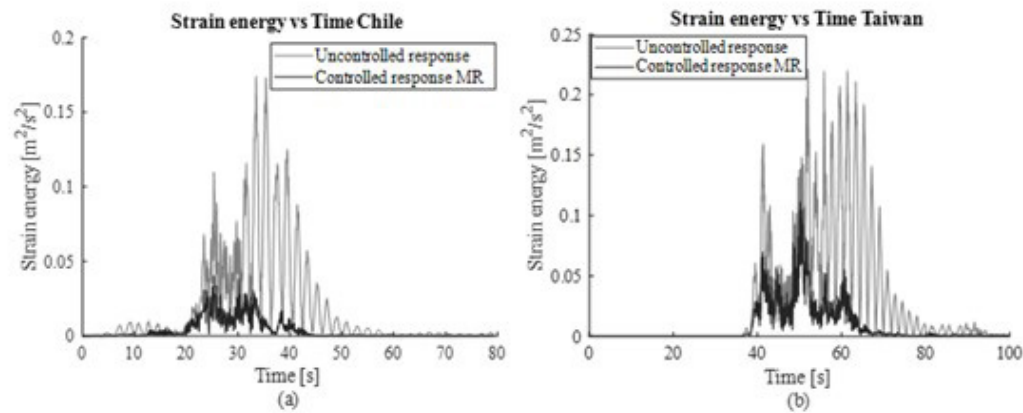


Figure 7. Strain Energy. (a) Strain Energy for Chile. (b) Strain Energy for Taiwan.

The results also show a reduction in the damping Energy. For the seismic excitation of Mexico, the average reduction was 57%, while in Petrolia, the average reduction was 39%. This demonstrates that the dissipation of the damping energy was effective, as shown in Figure (8).

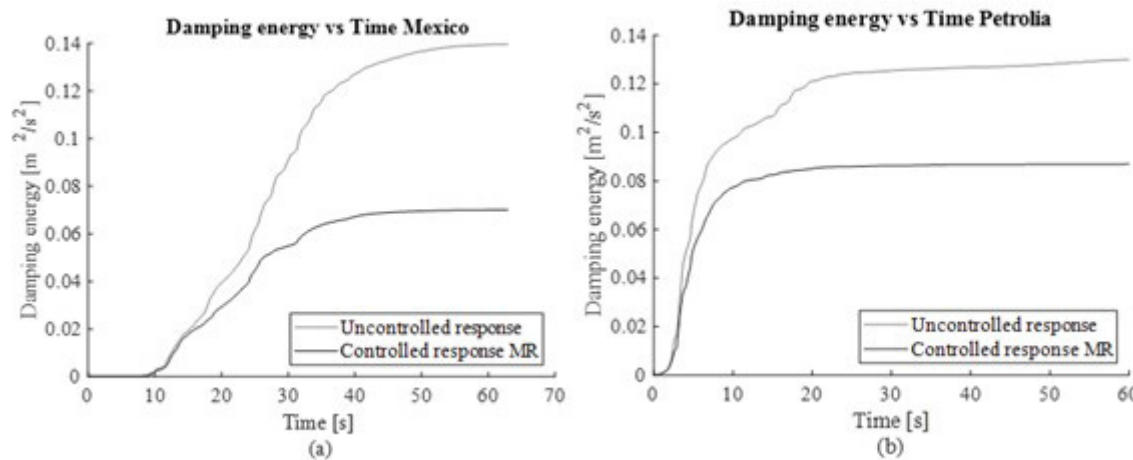


Figure 8. Damping Energy. (a) Damping Energy for Mexico. (b) Damping Energy for Petrolia.

Finally, different results were obtained for the reduction of the Kinetic Energy. For Christchurch seismic excitation, the average reduction was 62%, while in Morgan Hill, the reduction was 23%. Figure (9) demonstrates that the dissipation of Kinetic Energy was effective.

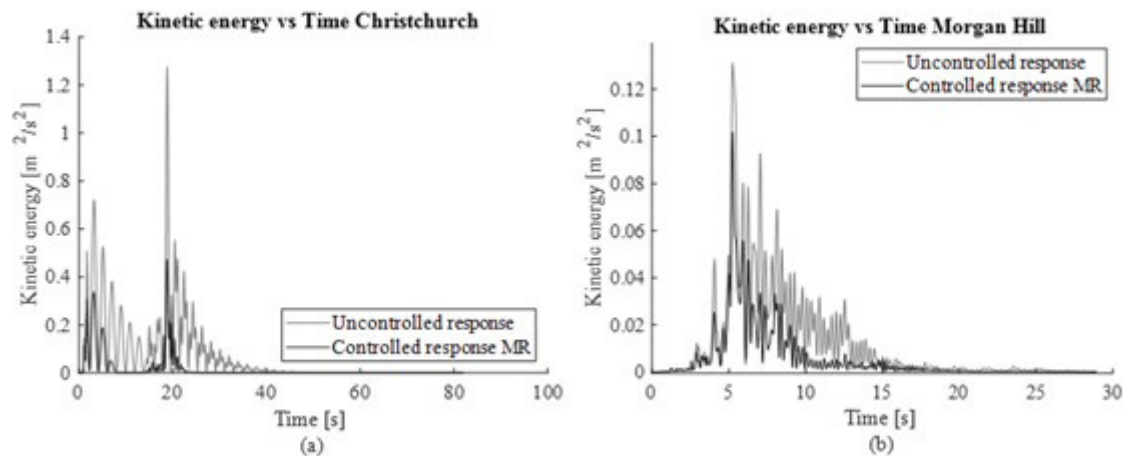


Figure 9. Kinetic Energy. (a) Kinetic Energy for Christchurch. (b) Kinetic Energy for Morgan Hill.

## Conclusions

The integration of an MR damper with FLC using optimized parameters through the WOA has shown significant effectiveness in enhancing the structural response to a wide range of seismic events.

This control system results in a significant reduction of displacement (up to 68%), velocity (up to 42%), acceleration (up to 12%), interstory drift (up to 42%), and RMS value of displacement (up to 75%) when compared to uncontrolled structures.

This improved performance plays a significant role in mitigating potential damage and ensuring the safety of structures subjected to dynamic loads.

This control system can adapt to the different characteristics of the seismic excitations. This adaptability is proved by the different requirements for the scaling factors  $k_d$  and  $k_v$  in response to different seismic events. This flexibility in adjusting the parameters improves the optimization results for each excitation and increases the effectiveness of the MR damper controlling the structural responses.

The energy dissipation analysis has become a reliable method to evaluate the effectiveness of the control system. The MR damper dissipates more energy than the uncontrolled cases, showing its efficacy in reducing the total impact of seismic forces on the structure. This energy dissipation mechanism is a key factor in limiting structural damage and ensuring the safety of the structure.

### CRedit authorship contribution statement

**Veronica Valencia Valencia:** conceptualization, Data curation, Formal analysis, Investigation, Methodology, Project administration, Resources, Software, Visualization, Writing – review & editing, Writing – original draft. **Luis A. Lara-Valencia:** conceptualization, Supervision, Validation, Writing – review & editing.

### Financing

The authors declare that the preparation of this research was not funded.



## Conflict of interest

The authors declare that they did not receive resources for the writing or publication of this article.

## Ethical implications

The authors do not have any type of ethical involvement that should be declared in the writing and publication of this article.

## References

1. Saaed TE, Nikolakopoulos G, Jonasson JE, Hedlund H. A state-of-the-art review of structural control systems. Vol. 21, *JVC/Journal of Vibration and Control*. SAGE Publications Inc.; 2015. p. 919-37. <https://doi.org/10.1177/1077546313478294>
2. Priya SD, K UP, Iyer NR. Enhancing the Seismic Response of Buildings with Energy Dissipation Methods-An Overview. *Journal of Civil Engineering Research [Internet]*. 2014;2014(2A):17-22. Available from: <http://journal.sapub.org/jce>
3. Casciati F, Rodellar J, Yildirim U. Active and semi-active control of structures-theory and applications: A review of recent advances. Vol. 23, *Journal of Intelligent Material Systems and Structures*. 2012. p. 1181-95. <https://doi.org/10.1177/1045389X12445029>
4. Bitaraf M, Ozbulut OE, Hurlebaus S, Barroso L. Application of semi-active control strategies for seismic protection of buildings with MR dampers. *Eng Struct*. 2010 Oct;32(10):3040-7. <https://doi.org/10.1016/j.engstruct.2010.05.023>
5. Lavasani SHH, Doroudi R. Meta heuristic active and semi-active control systems of high-rise building. *International Journal of Structural Engineering*. 2020;10(3):232-53. <https://doi.org/10.1504/IJSTRUCTE.2020.108529>
6. Hiramoto K, Matsuoka T, Sunakoda K. Simultaneous optimal design of the structural model for the semi-active control design and the model-based semi-active control. *Struct Control Health Monit*. 2014;21(4):522-41. <https://doi.org/10.1002/stc.1581>
7. Arash Bahar. HIERARCHICAL SEMIACTIVE CONTROL OF BASE-ISOLATED STRUCTURES. Barcelona; 2009 Apr. <https://doi.org/10.23919/ECC.2009.7074546>
8. Lara L, Brito J, Valencia Y. Comparative analysis of semi-active control algorithms applied to magnetorheological dampers. *Ingeniare Revista chilena de ingenieria*. 2017;25:39-58. <https://doi.org/10.4067/S0718-33052017000100039>
9. Fisco NR, Adeli H. Smart structures: Part I - Active and semi-active control. Vol. 18, *Scientia Iranica*. Sharif University of Technology; 2011. p. 275-84. <https://doi.org/10.1016/j.scient.2011.05.034>
10. Lara L, Brito J, Yamile V. REDUCTION OF VIBRATIONS IN A BUILDING USING MAGNETORHEOLOGICAL DAMPERS. 2012;79:205-14.
11. Yazid IIM, Mazlan SA, Kikuchi T, Zamzuri H, Imaduddin F. Design of magnetorheological damper with a combination of shear and squeeze modes. *Mater Des*. 2014;54:87-95. <https://doi.org/10.1016/j.matdes.2013.07.090>
12. Das D, Datta TK, Madan A. Semiactive fuzzy control of the seismic response of building frames with MR dampers. *Earthq Eng Struct Dyn*. 2012;41(1):99-118. <https://doi.org/10.1002/eqe.1120>





13. Dyke SJ, Spencer BF, Sain MK, Carlson JD. Seismic Response Reduction Using Magnetorheological Dampers. *IFAC Proceedings Volumes*. 1996 Jun;29(1):5530-5. [https://doi.org/10.1016/S1474-6670\(17\)58562-6](https://doi.org/10.1016/S1474-6670(17)58562-6)
14. F Spencer Jr BB, Dyke SJ, Member A, Sain MK, Carlson JD. Phenomenological model for Magnetorheological dampers [Internet]. 1997. Available from: <http://www.rheonetic.com/mrfluid> [https://doi.org/10.1061/\(ASCE\)0733-9399\(1997\)123:3\(230\)](https://doi.org/10.1061/(ASCE)0733-9399(1997)123:3(230))
15. Kwok NM, Ha QP, Nguyen MT, Li J, Samali B. Bouc-Wen model parameter identification for a MR fluid damper using computationally efficient GA. *ISA Trans*. 2007;46(2):167-79. <https://doi.org/10.1016/j.isatra.2006.08.005>
16. Guo S, Yang S, Pan C. Dynamic modeling of magnetorheological damper behaviors. *J Intell Mater Syst Struct*. 2006 Jan;17(1):3-14. <https://doi.org/10.1177/1045389X06055860>
17. Bathaei A, Zahrai SM, Ramezani M. Semi-active seismic control of an 11-DOF building model with TMD+MR damper using type-1 and -2 fuzzy algorithms. *JVC/Journal of Vibration and Control*. 2018 Jul 1;24(13):2938-53. <https://doi.org/10.1177/1077546317696369>
18. Lara L, Brito J, Graciano Gallego CA. Structural control strategies based on magnetorheological dampers managed using artificial neural networks and fuzzy logic. *Revista UIS Ingenierías [Internet]*. 2017 Sep 1;16(2):227-42. Available from: <http://revistas.uis.edu.co/index.php/revistausingenierias/article/view/6292/7075> <https://doi.org/10.18273/revuin.v16n2-2017021>
19. Rahman M, Ong ZC, Julai S, Ferdaus MM, Ahamed R. A review of advances in magnetorheological dampers: their design optimization and applications. Vol. 18, *Journal of Zhejiang University: Science A*. Zhejiang University; 2017. p. 991-1010. <https://doi.org/10.1631/jzus.A1600721>
20. Xia PQ. An inverse model of MR damper using optimal neural network and system identification. *J Sound Vib*. 2003 Oct 2;266(5):1009-23. [https://doi.org/10.1016/S0022-460X\(02\)01408-6](https://doi.org/10.1016/S0022-460X(02)01408-6)
21. Khalid M, Yusof R, Joshani M, Selamat H, Joshani M. Nonlinear identification of a magneto-rheological damper based on dynamic neural networks. *Computer-Aided Civil and Infrastructure Engineering*. 2014 Mar;29(3):221-33. <https://doi.org/10.1111/mice.12005>
22. Wei S, Wang J, Ou J. Method for improving the neural network model of the magnetorheological damper. *Mech Syst Signal Process*. 2021 Feb 15;149. <https://doi.org/10.1016/j.ymssp.2020.107316>
23. K-Karamodin A, H-Kazemi H. Semi-active control of structures using neuro-predictive algorithm for MR dampers. *Struct Control Health Monit*. 2010 Apr;17(3):237-53.
24. Uz ME, Hadi MNS. Optimal design of semi active control for adjacent buildings connected by MR damper based on integrated fuzzy logic and multi-objective genetic algorithm. *Eng Struct*. 2014 Jun 15;69:135-48. <https://doi.org/10.1016/j.engstruct.2014.03.006>
25. Braz-César M, Barros R. Optimization of a Fuzzy Logic Controller for MR Dampers Using an Adaptive Neuro-Fuzzy Procedure. *International Journal of Structural Stability and Dynamics*. 2017 Jun 1;17(5). <https://doi.org/10.1142/S0219455417400077>
26. Nanthakumar AJD, Jancirani J. Design optimization of magnetorheological damper geometry using response surface method for achieving maximum yield stress. *Journal of Mechanical Science and Technology*. 2019 Sep 1;33(9):4319-29. <https://doi.org/10.1007/s12206-019-0828-6>
27. Ding Y, Zhang L, Zhu HT, Li ZX. A new magnetorheological damper for seismic control. *Smart Mater Struct*. 2013 Nov;22(11). <https://doi.org/10.1088/0964-1726/22/11/115003>
28. Wani ZR, Tantray M, Sheikh JI. Experimental and numerical studies on multiple response optimization-based control using iterative techniques for magnetorheological damper-controlled structure. *Structural Design of Tall and Special Buildings*. 2021 Sep 1;30(13). <https://doi.org/10.1002/tal.1884>



29. Das D, Datta TK, Madan A. Semiactive fuzzy control of the seismic response of building frames with MR dampers. *Earthq Eng Struct Dyn*. 2012;41(1):99-118. <https://doi.org/10.1002/eqe.1120>
30. De Leon-Aldaco SE, Calleja H, Aguayo Alquicira J. Metaheuristic Optimization Methods Applied to Power Converters: A Review. *IEEE Trans Power Electron*. 2015 Dec 1;30(12):6791-803. <https://doi.org/10.1109/TPEL.2015.2397311>
31. Rasdi Rere LM, Fanany MI, Arymurthy AM. Metaheuristic Algorithms for Convolution Neural Network. *Comput Intell Neurosci*. 2016;2016. <https://doi.org/10.1155/2016/1537325>
32. Dokeroglu T, Sevinc E, Kucukyilmaz T, Cosar A. A survey on new generation metaheuristic algorithms. *Comput Ind Eng*. 2019 Nov 1;137. <https://doi.org/10.1016/j.cie.2019.106040>
33. Gandomi AH, Yang XS, Alavi AH, Talatahari S. Bat algorithm for constrained optimization tasks. *Neural Comput Appl*. 2013 May 1;22(6):1239-55. <https://doi.org/10.1007/s00521-012-1028-9>
34. Chakri A, Khelif R, Benouaret M, Yang XS. New directional bat algorithm for continuous optimization problems. *Expert Syst Appl*. 2017 Mar 1;69:159-75. <https://doi.org/10.1016/j.eswa.2016.10.050>
35. Bekdağ G, Nigdeli SM, Yang XS. A novel bat algorithm based optimum tuning of mass dampers for improving the seismic safety of structures. *Eng Struct*. 2018 Mar 15;159:89-98. <https://doi.org/10.1016/j.engstruct.2017.12.037>
36. Kumar A, Pant S, Ram M. System Reliability Optimization Using Gray Wolf Optimizer Algorithm. *Qual Reliab Eng Int*. 2017 Nov 1;33(7):1327-35. <https://doi.org/10.1002/qre.2107>
37. Kamgar R, Samea P, Khatibinia M. Optimizing parameters of tuned mass damper subjected to critical earthquake. *Structural Design of Tall and Special Buildings*. 2018 May 1;27(7). <https://doi.org/10.1002/tal.1460>
38. Kamgar R, Gholami F, Zarif Sanayei HR, Heidarzadeh H. Modified Tuned Liquid Dampers for Seismic Protection of Buildings Considering Soil-Structure Interaction Effects. *Iranian Journal of Science and Technology - Transactions of Civil Engineering*. 2020 Mar 1;44(1):339-54. <https://doi.org/10.1007/s40996-019-00302-x>
39. Takin K, Doroudi R, Doroudi S. Vibration control of structure by optimising the placement of semi-active dampers and fuzzy logic controllers. *Australian Journal of Structural Engineering*. 2021;22(3):222-35. <https://doi.org/10.1080/13287982.2021.1957198>
40. Mirjalili S, Lewis A. The Whale Optimization Algorithm. *Advances in Engineering Software*. 2016 May 1;95:51-67. <https://doi.org/10.1016/j.advengsoft.2016.01.008>
41. Lin X, Lin W. Whale Optimization Algorithm-Based LQG-Adaptive Neuro-Fuzzy Control for Seismic Vibration Mitigation with MR Dampers. *Shock and Vibration*. 2022 Mar 28;2022:1-21. <https://doi.org/10.1155/2022/4060660>
42. Lin X, Lin W. Optimal Allocation and Control of Magnetorheological Dampers for Enhancing Seismic Performance of the Adjacent Structures Using Whale Optimization Algorithm. *Shock and Vibration*. 2021;2021. <https://doi.org/10.1155/2021/1218956>
43. Rosli R, Mohamed Z. Optimization of modified Bouc-Wen model for magnetorheological damper using modified cuckoo search algorithm. *JVC/Journal of Vibration and Control*. 2021 Sep 1;27(17-18):1956-67. <https://doi.org/10.1177/1077546320951383>
44. Zabihi-Samani M, Ghanooni-Bagha M. Optimal Semi-active Structural Control with a Wavelet-Based Cuckoo-Search Fuzzy Logic Controller. *Iranian Journal of Science and Technology - Transactions of Civil Engineering*. 2019 Dec 1;43(4):619-34. <https://doi.org/10.1007/s40996-018-0206-0>

45. Rosli R, Mohamed MZ, Priyandoko G, Rashid MFFA. Bouc-Wen hysteresis parameter optimization for magnetorheological damper using Cuckoo search algorithm. In: AIP Conference Proceedings. American Institute of Physics Inc.; 2020. <https://doi.org/10.1063/5.0027238>
46. Rosli R, Mohamed MZ, Priyandoko G, Rashid MFFA. Bouc-Wen hysteresis parameter optimization for magnetorheological damper using Cuckoo search algorithm. In: AIP Conference Proceedings. American Institute of Physics Inc.; 2020. <https://doi.org/10.1063/5.0027238>
47. Valencia-Valencia V, Castro-Osorio M, Vallejo-Paniagua D, Echavarría-Montaña S, Lara-Valencia LA. CONTROL OF STRUCTURES SUBJECTED TO DYNAMIC LOADS USING MAGNETORHEOLOGICAL DAMPERS. In: COMPDYN Proceedings. National Technical University of Athens; 2023. <https://doi.org/10.7712/120123.10741.20135>
48. Boreiry M, Ebrahimi-Nejad S, Marzbanrad J. Sensitivity analysis of chaotic vibrations of a full vehicle model with magnetorheological damper. *Chaos Solitons Fractals*. 2019 Oct 1;127:428-42. <https://doi.org/10.1016/j.chaos.2019.07.005>
49. Jung HJ, Spencer BF, Asce M, Lee IW. Control of Seismically Excited Cable-Stayed Bridge Employing Magnetorheological Fluid Dampers. Available from: <http://wusceel.cive.wustl.edu/>
50. Castro-Osorio M, Vallejo-Paniagua D, Valencia-Valencia V, Lara-Valencia LA, Blandón-Valencia JJ. OPTIMAL DESIGN OF A TUNED MASS DAMPER INERTER USING A WHALE OPTIMIZATION ALGORITHM FOR THE CONTROL OF BUILDINGS SUBJECTED TO GROUND ACCELERATIONS. In: COMPDYN Proceedings. National Technical University of Athens; 2023. <https://doi.org/10.7712/120123.10743.20231>
51. Azizi M, Ejlali RG, Mousavi Ghasemi SA, Talatahari S. Upgraded Whale Optimization Algorithm for fuzzy logic based vibration control of nonlinear steel structure. *Eng Struct*. 2019 Aug 1;192:53-70. <https://doi.org/10.1016/j.engstruct.2019.05.007>
52. Wadood A, Khurshaid T, Farkoush SG, Yu J, Kim CH, Rhee SB. Nature-inspired whale optimization algorithm for optimal coordination of directional overcurrent relays in power systems. *Energies (Basel)*. 2019;12(12). <https://doi.org/10.3390/en12122297>
53. Lara-Valencia LA, Caicedo D, Valencia-Gonzalez Y. A novel whale optimization algorithm for the design of tuned mass dampers under earthquake excitations. *Applied Sciences (Switzerland)*. 2021 Jul 1;11(13). <https://doi.org/10.3390/app11136172>
54. Gharehchopogh FS, Gholizadeh H. A comprehensive survey: Whale Optimization Algorithm and its applications. *Swarm Evol Comput*. 2019 Aug 1;48:1-24. <https://doi.org/10.1016/j.swevo.2019.03.004>
55. Gupta MM. Forty-five years of fuzzy sets and fuzzy logic-A tribute to professor Lotfi A. Zadeh (the father of fuzzy logic). Vol. 18, *Scientia Iranica*. Sharif University of Technology; 2011. p. 685-90. <https://doi.org/10.1016/j.scient.2011.04.023>
56. Liu Y, Gordaninejad F, Evrensel CA, Hitchcock G. An Experimental Study on Fuzzy Logic Vibration Control of a Bridge Using Fail-Safe Magneto-Rheological Fluid Dampers [Internet]. 2001. Available from: <http://Web.me.unr.edu/ciml> <https://doi.org/10.1117/12.434135>
57. Lara-Valencia LA, Valencia-Gonzalez Y, Luis Vital De Brito J. Use of fuzzy logic for the administration of a structural control system based on magnetorheological dampers. Vol. 74, *Rev. Fac. Ing. Univ. Antioquia N*. 2015. <https://doi.org/10.17533/udea.redin.16461>
58. Sun Y, Yang T, Liu Z. A whale optimization algorithm based on quadratic interpolation for high-dimensional global optimization problems. *Applied Soft Computing Journal*. 2019 Dec 1;85. <https://doi.org/10.1016/j.asoc.2019.105744>



59. Jung HJ, Spencer BF, Asce M, Lee IW. Control of Seismically Excited Cable-Stayed Bridge Employing Magnetorheological Fluid Dampers. Available from: <http://wusceel.cive.wustl.edu/>

60. Center for engineering strong-motion data (CESMD) [Internet]. [cited 2022 Dec 25]. Available from: [www.strongmotioncenter.org](http://www.strongmotioncenter.org).